

Energy and angular-momentum balance in wall-bounded superfluid turbulence

J.J. Hosio,^{1,*} V.B. Eltsov,¹ P.J. Heikkinen,¹ M. Krusius,¹ and V.S. L'vov²

¹*O.V. Lounasmaa Laboratory, P.O. Box 15100, FI-00076 AALTO, Finland*

²*Department of Chemical Physics, The Weizmann Institute of Science, Rehovot 76100, Israel*

(Dated: August 14, 2012)

An example of steady-state wall-bounded quantum turbulence is provided by the turbulent vortex front. In a rotating cylinder filled with originally vortex-free superfluid $^3\text{He-B}$, the front propagates axially and sets the superfluid in rotation. Our measurements of the front propagation at different angular velocities and temperatures down to $0.16T_c$ show that besides the energy-dissipation mechanisms, the transfer of angular momentum is increasingly important for the turbulent dynamics in the $T \rightarrow 0$ limit. We suggest a phenomenological model that describes the front velocity in terms of two effective mutual-friction parameters, which govern the energy and momentum balance, respectively. The residual values of these parameters in the $T \rightarrow 0$ limit differ by two orders of magnitude. In this limit, the efficient energy dissipation can be associated in traditional manner with the turbulent energy cascade toward small length scales, while the much less effective angular-momentum transfer causes decoupling of the superfluid from the rotating container.

PACS numbers: 67.30hb, 47.15.ki, 47.20.-k, 67.25.dk

Introduction:—The new frontier of superfluid dynamics is the limit where the density of normal excitations tends to zero, on approaching zero temperature. There all traditional dissipation mechanisms in vortex flow rapidly vanish, extrapolations of the hydrodynamics from higher temperatures in terms of the superfluid Reynolds number predict increasing tendency towards turbulence, and the situation is reminiscent of what is known as the viscous anomaly in the turbulence of viscous fluids. This limit has been studied in both superfluid ^4He and $^3\text{He-B}$ with the focus on the dissipation rate, i.e., on the energy transfer from the superfluid to the normal component [1–3]. Here we consider also the coupling of the superfluid to its container, i.e., the angular-momentum transfer to the superfluid component in a rapid increase of rotation in an axially symmetric container, the so-called spin-up.

In classical viscous fluids, the spin-up response is dominated by surface interactions and characterized by the creation of the Ekman boundary layer [4]. The details of the dynamics are affected by turbulent, nonlinear processes [5]. In the absence of quantized vortex lines, the superfluid component does not respond to the rotation of its container. This state in rotation is called the vortex-free Landau state. In the presence of vortices the transfer of angular momentum to the superfluid component is assisted by the mutual-friction force between the vortex lines and the normal-fluid excitations [6]. In superfluid ^4He , the small vortex-core diameter of order 1 \AA emphasizes the role of pinning of vortices at the container walls and vortex-boundary interactions [7, 8].

In $^3\text{He-B}$ contained in a smooth-walled cylinder, surface effects, such as vortex pinning, are strongly suppressed compared to superfluid ^4He , owing to the more than two orders of magnitude larger diameter of the vortex core. The spin-up responses at low temperatures, where the normal component consists of a dilute gas of

ballistic thermal excitations, can be divided into three categories: First, in the absence of remanent vortices, the superfluid remains free of vortices and thus irrotational up to angular velocities of a few rad/s depending on the wall roughness and the cylinder radius, while the normal component follows the rotation of the container due to diffuse wall scattering. Almost no kinetic energy or angular momentum is transferred to the fluid due to the negligible density of the normal fluid. Second, if the container walls are initially covered with a sufficient amount of remanent vortices, the spin-up takes place as laminar solid-body-like motion determined by the mutual-friction coupling in the bulk liquid [9]. In this case, the transfer rate of both energy and angular momentum decrease exponentially with temperature, unless some residual effects intervene, as observed in the laminar spin-down of Ref. [10].

Here we study a third possibility, in which the spin-up starts from localized turbulent vortex formation. This localized turbulent burst, started by remnants pinned on a rough sintered heat exchanger surface, leads to the formation of a vortex front propagating axially along a smooth-walled long quartz cylinder [2]. The azimuthally precessing and axially propagating front motion corresponds to an axially inhomogeneous spin-up of the superfluid component from rest (in the initial vortex-free Landau state at $\mathbf{v}_s = 0$) to a state with approximately solid-body rotation at a velocity $\mathbf{v}_s = \Omega_s \hat{\mathbf{z}} \times \mathbf{r}$ in the cylindrical coordinates (r, φ, z) . The front consists of a turbulent core with a size comparable to the cylinder radius and a bundle behind it which is approximately in solid-body rotation. Across the core, in which the vortices are bent to the side wall, the angular velocity changes from zero to Ω_s . This differential precession winds the vortex lines to a twisted configuration which extends from the front to the vortex bundle behind it [11].

At sufficiently high temperatures, above $0.4T_c$, mutual friction provides the coupling between the reference frame of the container and the rotating frame of the superfluid so that excluding the twist, the superfluid behind the front is at rest in the container frame. The coupling between the frames decreases with decreasing temperature as the normal fluid density is reduced exponentially in the $T \rightarrow 0$ limit. Bolometric measurements at $0.20T_c$ supported by numerical simulations in Ref. [12] showed the density of the vortices behind the front to fall well below the equilibrium value and the front propagation to be followed by a slow laminar spin-up of the superfluid.

Here we present new extensive measurements and analysis of the decoupling in terms of the transfer rate of energy and angular momentum inferred from the propagation velocity of the turbulent vortex front both as a function of temperature and rotation velocity Ω of the container. With adequate thermal contact between the superfluid sample and the heat exchanger, one can study the transfer properties down to the limit where the spin-up response becomes practically independent on temperature.

Phenomenological model:—At temperatures above $0.5T_c$, front motion is laminar and its velocity is determined by the mutual-friction dissipation $\alpha(T)$,

$$V_f \approx \alpha(T)\Omega R, \quad (1)$$

where Ω is the rotation velocity, and R the radius of the cylindrical container [13]. At lower temperatures, where the dissipative mutual-friction parameter decreases as [14]

$$\alpha(T) = \beta \exp(-\Delta/T), \quad (2)$$

the front motion starts to deviate from the laminar behavior (1) due to the extra dissipation provided by turbulent processes [2]. Here β is a pressure-dependent constant and Δ is the pressure- and temperature-dependent superfluid energy gap. In the simplest model of the front, the vortex state behind the thin front is in solid-body-like rotation with the angular velocity $\Omega_s \approx \Omega$.

At low temperatures, the helically twisted vortex bundle behind the front is in a quasiequilibrium state at the reduced velocity $\Omega_s \leq \Omega$ [12]. In analogy with the high-temperature behavior (Eq. 1), with Ω replaced by Ω_s , one may suggest that

$$V_f \approx \alpha_{\text{eff}}(T)\Omega_s R, \quad (3)$$

where the effective mutual-friction parameter $\alpha_{\text{eff}}(T)$ is the sum of a term proportional to the mutual-friction parameter and a turbulent-induced term, i.e.,

$$\alpha_{\text{eff}}(T) = C\alpha(T) + \alpha_{\text{turb}}. \quad (4)$$

Here C is a constant close to unity and for simplicity, α_{turb} is assumed to be independent both of temperature and rotation velocity.

Our decoupling model considers the angular-momentum balance of the rotating superfluid in terms of a course-grained hydrodynamical equation for the superfluid velocity \mathbf{v}_s , which is given by

$$\frac{\partial \mathbf{v}_s}{\partial t} + \nabla \mu - \mathbf{v}_s \times (\nabla \times \mathbf{v}_s) = \mathbf{F}_\alpha + \mathbf{F}_\lambda. \quad (5)$$

Here μ is the chemical potential. The two forces on the right-hand side are the mutual-friction force between the superfluid and the normal-fluid components with velocities \mathbf{v}_s and \mathbf{v}_n ,

$$\mathbf{F}_\alpha = -\alpha \hat{\omega} \times ((\mathbf{v}_s - \mathbf{v}_n) \times (\nabla \times \mathbf{v}_s)), \quad (6)$$

and the force due to line tension [15],

$$\mathbf{F}_\lambda = -\lambda (\nabla \times \mathbf{v}_s) \times (\nabla \times \hat{\omega}). \quad (7)$$

The unit vector $\hat{\omega}$ is directed along the vorticity $\nabla \times \mathbf{v}_s$. The line-tension parameter λ depends on the intervortex distance $\ell = \sqrt{\kappa/2\Omega}$ and the vortex core diameter a as

$$\lambda = (\kappa/4\pi) \ln(\ell/a), \quad (8)$$

where $\ell \sim 0.1$ mm, a is comparable to the superfluid coherence length $\xi \approx 70$ nm at 0.5 bar liquid pressure, and $\kappa \approx 0.07$ mm²/s is the circulation quantum.

In equilibrium, the global force balance dictates $\langle F_\alpha \rangle = \langle F_\lambda \rangle$ for the azimuthal components F_α and F_λ . With the simple estimate $\nabla \times \mathbf{v}_s \simeq 2\Omega_s$ one obtains

$$\langle F_\alpha \rangle \simeq 2\alpha\Omega_s(\Omega - \Omega_s)R. \quad (9)$$

The azimuthal line-tension force vanishes in the solid-body approximation. However, since the vortex state is twisted, the vorticity ω is not perfectly parallel with \hat{z} . The twist is proportional to Ω_s and has to be normalized by ΩR , i.e., $\nabla \times \hat{\omega} \simeq \Omega_s/(\Omega R)$ yielding

$$\langle F_\lambda \rangle \simeq 2\lambda\Omega_s^2/(\Omega R). \quad (10)$$

The solid-body-like angular velocity is obtained from the force balance equation

$$\alpha\Omega_s(\Omega - \Omega_s)R = \lambda\Omega_s^2/(\Omega R). \quad (11)$$

Due to the approximative nature of Eqs. (9) and (10), we replace the mutual friction parameter $\alpha(T)$ in Eq. (11) with a new mutual-friction parameter $\alpha_{\text{am}}(T)$ for angular momentum,

$$\alpha_{\text{am}} = C_{\text{am}}\alpha(T) + \alpha_{\text{res}}, \quad (12)$$

where C_{am} is a constant of the order of unity and the constant α_{res} accounts for possible temperature-independent residual effects related to the angular-momentum transfer. Solving Eq. (11) for Ω_s yields

$$\Omega_s = \frac{\alpha_{\text{am}}}{\alpha_{\text{am}}\Omega + \lambda R^{-2}}\Omega^2. \quad (13)$$

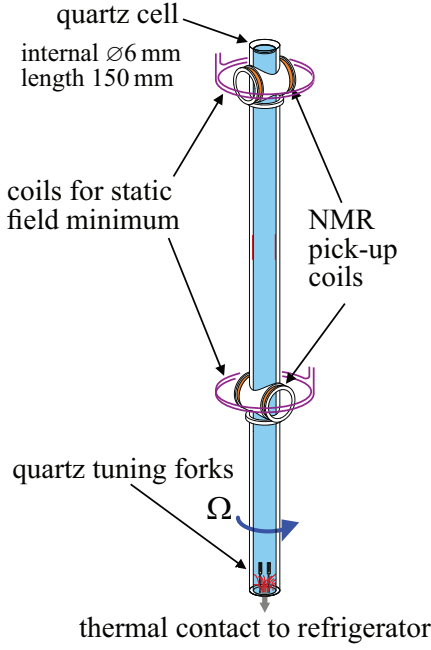


FIG. 1. The experimental setup. The ^3He -B sample is contained in a 15-cm-long quartz cylinder with 6 mm inner diameter. The front motion is triggered by a rapid increase of the rotation velocity Ω which leads to the creation of vortices in the heat exchanger volume. The upward-propagating front is detected with two NMR pick-up coils, which are 9 cm apart. The quartz tuning forks at the bottom are used for thermometry.

In Ref. [12] this result was written in terms of the two Reynolds numbers $\text{Re}_\alpha \approx 1/\alpha(T)$ and $\text{Re}_\lambda \sim \Omega R^2/\lambda$. In our case, the former controls the spin-up due to the coupling to the normal component, while the latter describes the tendency of the superfluid to decrease the vortex number due to the vortex-line tension between the vortices in the front and the bundle behind it. Setting $\alpha_{\text{am}} = \alpha$ in Eq. (13), we get a simple interpolation formula in terms of the two Reynolds numbers [12]

$$\Omega_s/\Omega = (1 + \text{Re}_\alpha/\text{Re}_\lambda)^{-1}. \quad (14)$$

However here, making use of (3), we fit the measurements to the more extended model

$$V_f = (C\alpha + \alpha_{\text{turb}}) \frac{C_{\text{am}}\alpha + \alpha_{\text{res}}}{(C_{\text{am}}\alpha + \alpha_{\text{res}})\Omega + \lambda R^{-2}} \Omega^2 R. \quad (15)$$

Experimental techniques:—Our experimental setup (Fig. 1) consists of a long quartz cylinder filled with liquid ^3He at 0.5 bar pressure. At its bottom end, the sample tube opens to a sintered-silver heat exchanger. Its rough surface ensures that vortices are formed there at low rotation velocity. In the experiment, we rapidly increase the rotation velocity from zero to the desired target velocity. This creates a turbulent burst at the bottom of the quartz tube and triggers an upward-propagating vortex front. Owing to the smooth walls, the critical velocity of vortex

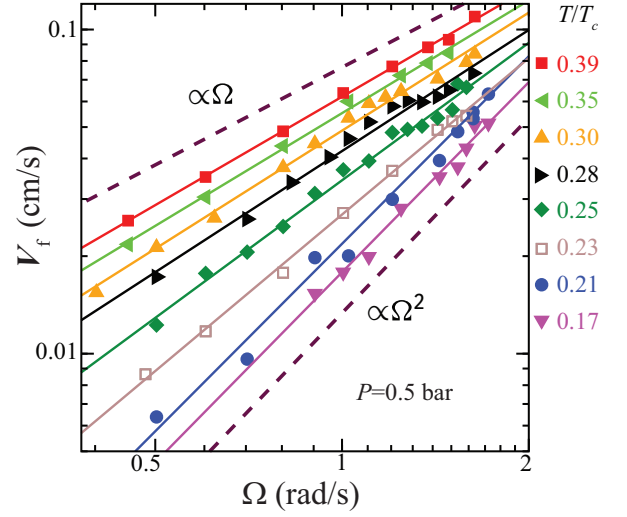


FIG. 2. Measured front velocity $V_f(T, \Omega)$ with logarithmic axes. The solid lines represent the velocity fitted to Eq. (15). At high temperatures, the Ω -dependence is linear, while in the zero-temperature limit the velocity tends to a quadratic dependence. The dashed lines correspond to $V_f \propto \Omega$ and $V_f \propto \Omega^2$ behavior for comparison.

formation is as high as 1.8 rad/s in the quartz tube and thus at lower velocities, the volume above the front remains in the meta-stable vortex-free Landau state, which eventually is displaced by the front.

The propagation is monitored with two NMR pick-up coils. At temperatures above $0.2T_c$, the arrival of the front can be detected by tracing the NMR signal at the so-called counterflow peak [13]. The arrival is seen as a rapid decrease of the NMR absorption. At the lowest rotation velocity of our measurements, $\Omega \approx 0.4$ rad/s, this detection method loses sensitivity at around $0.23T_c$, especially in the case of the coil at the top which operates at a smaller value of steady magnetic field. Even at our highest rotation velocity the counterflow peak becomes practically invisible below $0.18T_c$. There the front propagation can be monitored with the frequency shift of the magnon condensate in a magnetic trap in the middle of the pick-up coil, which depends strongly on the amount of local counterflow $\mathbf{v}_n - \mathbf{v}_s$ [16]. The small axial pinch coils around the NMR pick-up coils in Fig. 1 are used to provide the localization of the trap in the axial direction. Temperature is measured from the resonance width of a quartz tuning fork oscillator, which depends on temperature as $\Delta f = 11460 \text{ Hz} \exp(-1.776T_c/T)$ in the ballistic regime of quasiparticle transport.

After each measurement, the rotation is stopped and the sample is warmed up to $T \sim 0.7T_c$ for about one hour to allow the remanent vortices to annihilate [17] before cooling down again for a new measurement. Alternatively, the sample can be warmed up above T_c upon which it may be cooled down immediately.

Results:—Figure 2 shows the front velocity $V_f(T, \Omega)$

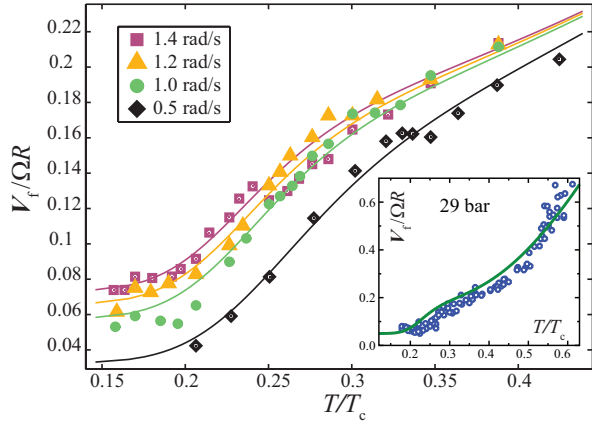


FIG. 3. The scaled front velocity $v_f = V_f/(\Omega R)$ as a function of temperature at four different rotation velocities. The solid lines indicate the velocity fitted to Eq. (15). In the zero-temperature limit the velocity tends to a temperature-independent but rotation-velocity-dependent constant value determined by the residual terms α_{turb} and α_{res} . The inset shows the scaled velocity data at 29 bar from Ref. [2] for $\Omega \approx 1$ rad/s. The solid line shows the predicted velocity from Eq. (15) using the same four parameter values obtained from the 0.5 bar measurements but with β and Δ replaced with their 29 bar values.

as a function of rotation velocity in the range $\Omega = 0.4 - 1.7$ rad/s at eight different temperatures ranging from 0.16 to $0.4 T_c$. In this temperature interval the mutual friction parameter α changes by roughly three orders of magnitude. At $0.4 T_c$ the front velocity follows the single-vortex model of Eq. (1) and the measured data points depend almost linearly on Ω . As expected from Eq. (15), the dependence gradually changes from linear toward quadratic at temperatures below $0.3 T_c$. As a function of temperature, the scaled front velocity at four different rotation velocities is shown in Fig. 3. This plot demonstrates that V_f at constant Ω becomes temperature independent below $0.2 T_c$ as reported in Ref. [2]. The new measurements reveal that the limiting scaled velocity increases with increasing Ω as expected from Eq. (15).

The fits in Figs. 2 and 3 use C , C_{am} , α_{turb} and α_{res} as common fitting parameters taking β from measurements in Ref. [10]. The obtained values are $C \approx 0.52$, $C_{\text{am}} \approx 1.33$, $\alpha_{\text{turb}} \approx 0.20$, and $\alpha_{\text{res}} \approx 0.0019$. The fitted curves are in reasonable agreement with the measured data and reproduce well the limiting behavior both in the high- and in the low-temperature limits. Additionally, small axial asymmetries in the precessing front and in the bundle behind it cause oscillations in the NMR signal, which allows us to measure Ω_s directly, albeit in a limited range of temperatures slightly above $0.2 T_c$. These measurements qualitatively agree with Eq. (14). Using the same four parameters in Eq. (15) produces a reasonable agreement with the data measured earlier at 29 bar in a different quartz container. This is demonstrated in the inset of Fig. 3. Thus, it seems that the

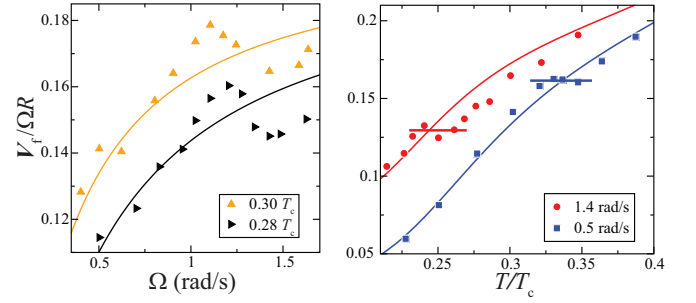


FIG. 4. Nonmonotonic features in the front velocity. The left panel shows a zoomed view of the scaled front velocity $v_f = V_f/(\Omega R)$ at temperatures 0.28 and $0.30 T_c$ illustrating the maxima at $\Omega=1-1.2$ rad/s. On the right is a zoomed view of the temperature dependence for two different rotation velocities showing plateaus at rotation-velocity-dependent temperatures. The solid lines show the velocity from Eq. (15) with the fitting parameters given in the text.

phenomenological parameters have no strong dependence on the vortex-core diameter.

The residual term of the angular-momentum transfer α_{res} is about four times larger but still comparable to the corresponding residual term observed for laminar vortex motion in Ref. [10]. The larger value is expected, since it reflects the additional residual processes induced by the turbulence in the front. In the turbulent front motion, the vortex ends move along the sidewall of the cylinder, which supposedly enhances the surface interactions and increases angular-momentum transfer, when compared to the motion of predominantly parallel vortex lines sliding along, e.g., the flat top quartz end plate of the sample tube in laminar vortex flow [10].

Importantly, α_{res} is still a factor of hundred smaller than the residual term α_{turb} describing the energy transfer in the turbulent energy cascade. This means that the turbulent processes effectively enhance the energy transfer and consequently, the front velocity becomes practically temperature independent below $0.2 T_c$. The angular-momentum transfer, however, is not efficiently enhanced by turbulence. With vanishing mutual friction, this leads to the observed quasiequilibrium solid-body-like rotation where the superfluid angular velocity $\Omega_s < \Omega$ depends strongly on rotation velocity.

At the intermediate temperatures, the velocity behaves in a peculiar manner at high Ω , namely, v_f is nonmonotonic with a temperature-dependent maximum at $\Omega=1-1.2$ rad/s as demonstrated in the left panel of Fig. 4. This is reflected as plateaus at rotation-velocity-dependent temperatures ranging from $0.24-0.26 T_c$ for 1.4 rad/s to $0.32-0.35 T_c$ for 0.5 rad/s as can be seen in the zoomed view of the temperature dependence in the right panel of Fig. 4. A possible explanation is the bottleneck accumulation of the kinetic energy that leads to plateaus in the temperature range where the energy cascade approaches the intervortex distance $\ell = \sqrt{\kappa/(2\Omega_s)}$ [2, 18, 19]. This

assumption is supported by the fact that the value of α_{eff} at the two plateaus decreases with increasing rotation velocity (see Fig. 4, right).

Discussion:—Our model qualitatively explains the observed front velocity in a wide region of angular velocities (0.4–1.7 rad/s) and temperatures (0.16–0.4 T_c). The origin of the observed residual term α_{turb} has been attributed to the energy transfer in the turbulent energy cascade and to reflect the phenomenon of anomalous dissipation [2]. Another recently suggested mechanism which could lead to temperature-independent dissipation in the zero-temperature limit is the leakage of quasiparticle excitations from overheated vortex cores due to the turbulence-induced Kelvin waves on vortex lines [20].

A new observation is the small value of the residual term α_{res} in comparison to α_{turb} . Consequently, in the zero-temperature limit angular momentum transfer becomes weak. Possibly surface interactions at the cylindrical wall, which have little effect at higher temperatures, play some role in the observed residual coupling.

Contrary to earlier indications [21], these measurements show that turbulence is not the inevitable dynamic response in the $T \rightarrow 0$ limit. New mechanisms help to promote laminar flow, like the partial decoupling from the applied rotation drive, followed by slow laminar recovery to the equilibrium state. Secondly, as already known from measurements of the decay of vortex tangles in superfluid ^4He and in $^3\text{He-B}$ [22], vortex flow at $T = 0$ is not dissipationless, but new sources of residual dissipation and friction are observed. The identification of these sources in both Bose and Fermi superfluids remains a task for the next near future.

The work is supported by the Academy of Finland (Centers of Excellence Programme 2012-2017), the EU 7th Framework Programme (FP7/2007-2013, grant 228464 Microkelvin), and the USA-Israel Binational Science Foundation. J.H. and P.H. acknowledge financial support from the Väisälä Foundation of the Finnish Academy of Science and Letters.

* jaakko.hosio@aalto.fi

- [1] D. I. Bradley, D. O. Clubb, S. N. Fisher, A. M. Guénault, R. P. Haley, C. J. Matthews, G. R. Pickett, V. Tsepelin, and K. Zaki, *Phys. Rev. Lett.* **96**, 035301 (2006).
- [2] V. B. Eltsov, A. I. Golov, R. de Graaf, R. Hänninen, M. Krusius, V. S. L'vov, and R. E. Solntsev, *Phys. Rev. Lett.* **99**, 265301 (2007).
- [3] P. M. Walmsley, A. I. Golov, H. E. Hall, A. A. Levchenko, and W. F. Vinen, *Phys. Rev. Lett.* **99**, 265302 (2007).
- [4] H. P. Greenspan, *The Theory of Rotating Fluids* (Cambridge University Press, Cambridge, 1968).
- [5] E. R. Benton and A. Clark, *Ann. Rev. Fluid Mech.* **6**, 257 (1974).
- [6] A. Reisenegger, *J. Low Temp. Phys.* **92**, 77 (1993).
- [7] P. W. Adams, M. Cieplak, and W. I. Glaberson, *Phys. Rev. B* **32**, 171 (1985).
- [8] I. Aranson and V. Steinberg, *Phys. Rev. B* **54**, 13072 (1996).
- [9] V. B. Eltsov, R. de Graaf, P. J. Heikkinen, J. J. Hosio, R. Hänninen, M. Krusius, and V. S. L'vov, *Phys. Rev. Lett.* **105**, 125301 (2010).
- [10] J. J. Hosio, V. B. Eltsov, M. Krusius, and J. T. Mäkinen, *Phys. Rev. B* **85**, 224526 (2012).
- [11] V. B. Eltsov, A. P. Finne, R. Hänninen, J. Kopu, M. Krusius, M. Tsubota, and E. V. Thuneberg, *Phys. Rev. Lett.* **96**, 215302 (2006).
- [12] J. J. Hosio, V. B. Eltsov, R. de Graaf, P. J. Heikkinen, R. Hänninen, M. Krusius, V. S. L'vov, and G. E. Volovik, *Phys. Rev. Lett.* **107**, 135302 (2011).
- [13] A. P. Finne, V. B. Eltsov, R. Blaauwgeers, Z. Janu, M. Krusius, and L. Skrbek, *J. Low Temp. Phys.* **134**, 375 (2004).
- [14] N. B. Kopnin, *Rep. Prog. Phys.* **65**, 1633 (2002).
- [15] R. Ostermeyer and W. Glaberson, *J. Low Temp. Phys.* **21**, 191 (1975).
- [16] S. Autti, Y. M. Bunkov, V. B. Eltsov, P. J. Heikkinen, J. J. Hosio, P. Hunger, M. Krusius, and G. E. Volovik, *Phys. Rev. Lett.* **108**, 145303 (2012).
- [17] V. B. Eltsov, R. de Graaf, P. J. Heikkinen, J. J. Hosio, R. Hänninen, and M. Krusius, *J. Low Temp. Phys.* **161**, 474 (2010).
- [18] V. S. L'vov, S. V. Nazarenko, and O. Rudenko, *Phys. Rev. B* **76**, 024520 (2007).
- [19] V. S. L'vov, S. V. Nazarenko, and O. Rudenko, *J. Low Temp. Phys.* **153**, 140 (2008).
- [20] M. A. Silaev, *Phys. Rev. Lett.* **108**, 045303 (2012).
- [21] A. P. Finne, T. Araki, R. Blaauwgeers, V. B. Eltsov, N. B. Kopnin, M. Krusius, L. Skrbek, M. Tsubota, and G. E. Volovik, *Nature* **424**, 1022 (2003).
- [22] W. F. Vinen, *J. Low Temp. Phys.* **161**, 419 (2010).